

# Investigation of air flow around buildings using computational fluid dynamics techniques

Appupillai Baskaran and Ahmed Kashef

*Building Performance Laboratory, Institute for Research in Construction, National Research Council Canada, Ottawa, Ontario, Canada, K1A 0R6*

The developments of the Computational Fluid Dynamics (CFD) method as a powerful tool for prediction of wind environmental conditions around buildings are presented in this study. CFD techniques have been applied in predicting wind flow conditions: around a single building, between two parallel buildings and around a multiple building configuration. Also presented is a limited model validation for those simulated configurations. Finally, the paper presents the application of CFD techniques for a case study in simulating an existing site together with proposed buildings and the local landscape. Crown Copyright © 1996 Published by Elsevier Science Ltd.

**Keywords:** computational fluid dynamics, air flow, buildings

## 1. Introduction

Understanding the air flow patterns around buildings is of importance for designing durable building envelopes. Model scale buildings and structures have been tested in simulated flow established in boundary layer wind tunnels (BLWT). In 1956, the first successful attempt was made by Cermak and tests were performed on the World Trade Center model which marks the first use of the BLWT for building design. Physical modeling techniques were also extended to the solution of various problems such as the study of mountain-valley winds<sup>1</sup> and wind-wave interactions<sup>2</sup>. These advancements made many important contributions to the field of wind engineering.

BLWT studies have been a great source of information for updating the building codes and standards of practice<sup>3</sup>.

The method of dimensional analysis is a common procedure in relating model-test results to the full-scale performance. For the BLWT to predict the behavior of the full-scale prototype in the natural wind, the relevant physical properties of both the structure and of the atmospheric boundary layer must be properly represented in the model. Thus, to achieve complete similarity between the model and the prototype, a number of non-dimensional parameters, such as Reynolds and Froude numbers, have to match. In practice it is rarely possible to satisfy all these non-dimensional parameters. For example, the conditions imposed by the individual parameters are incompatible and, in general, no material with the physical properties demanded for the similarity requirement is available for model construction<sup>4</sup>.

This implies the satisfaction of only a few similarity parameters. The selection of the similarity parameters to be satisfied in any particular study depends upon the nature of the problem. Thus it is necessary to introduce compromise procedures which in turn introduce uncertainties in the interpretation of the model results, yet it still permits the relevant data to be obtained.

Generally, BLWT may yield overestimated results because of the extraneous suction effects introduced into the wake due to the proximity of the tunnel walls<sup>4</sup>. The extent of this overestimation depends primarily on the proportion of the tunnel cross-section area occupied by the model and on whether the flow over the model is attached or separated. Therefore, it is always recommended to limit the size of the model to less than 5% of the area of the working section of the wind tunnel. In other cases of larger models the use of corrections for the wake blockage is unavoidable. High cost, restricted data potential of field studies and long time requirements have severely limited prototype measurements.

Advancements in computational fluid dynamics (CFD) and numerical modeling techniques provide new approaches to quantify building air flow. This paper presents the application of CFD for modeling wind environmental conditions around a variety of building configurations. Examined configurations include: wind flow around a single building, flow between parallel buildings and air flow around multiple building configurations. First, computed flow fields are presented for the above configurations to demonstrate the inherent advantages of CFD, such as its

ability in providing detailed information about the flow field while modeling the complexities induced in the flow domain. Second, model validation is performed by post processing the computed results and comparing them with the available limited experimental data. In addition, the paper also presents the computed results from a case study for which the CFD technique is applied as a predictive tool during the design stage. The case study simulation not only accounts for modeling the buildings, but also, for the first time, attempts have been made to simulate the surrounding landscape such as the hills and trees. The simulated results of the case study are displayed by selecting images from an animation process that has also been developed as a part of the present investigation.

## Notation

$B$	building width ( $x$ )
$DS1, DS2$	distances from the building side across the flow—along $x$ direction
$DSD$	down-stream distance
$DT$	distance from the building top
$H$	height of the building ( $y$ )
$I$	width of the passage between buildings
$k$	fluid kinetic energy
$L$	building length ( $z$ )
$I_R$	length of the recirculation zone
$U$	mean velocity, $\sqrt{u^2+v^2+w^2}$
$U_n$	wind velocity used for normalization
$USD$	up-stream distance
$U_s$	free stream velocity
$u, v, w$	mean velocity components along $x, y, z$ directions
$x, y, z$	distance along the coordinate axis

## 2. Investigation of the computed wind flow field

This section presents and discusses the computed wind flow field around various simulated building configurations. Preceding that, a brief description of the applied solution methodology is included.

### 2.1. Applied solution methodology

Basically, the current solution methodology consists of three main steps: pre-processing, main computation and post-processing. A modular structure computer code, TWIST—turbulent wind simulation technique—has been developed to compute air flow around buildings<sup>5</sup>. The code is in FORTRAN and it is capable of running under a variety of platforms such as IBM-3090 (7 MFlops), HP 735 (36 MIPS) and even on micros from 286 PC or higher. TWIST simulated various wind flow conditions and they are reported in Baskaran and Stathopoulos<sup>6</sup>, Stathopoulos and Baskaran<sup>7</sup> and Baskaran and Stathopoulos<sup>8,9</sup>. For the present study, TWIST is used to evaluate the wind environmental conditions around single and two building models.

For the investigation of multiple building configuration as well as the case study, the well-known CFD solver PHOENICS<sup>10</sup> is used. Besides the customizing procedures, two major sub modules are needed to use PHOENICS for wind flow modeling. They are:

- input module, known as Q1 file, consisting of computational domain sizes, details for grid arrangement, coor-

dinates for building locations and other computational parameters such as values for initial flow conditions, convergence criteria and relaxation factors;

- boundary module, known as GROUND, consists of boundary specification, selection of necessary numerical schemes and turbulence models.

Details of these two major modifications are reported in Baskaran<sup>11</sup> and CHAM<sup>12</sup>.

Both codes use the control volume method (CVM), which has been demonstrated as a successful numerical procedure in many areas of computational wind engineering. CVM is used to convert the non-linear partial differential equations into difference equations. Solution of the difference equations is obtained at several thousand control volume nodes such that the satisfaction of the momentum transferred between the control volumes is guaranteed at steady state conditions. To fulfill the continuity of mass, the well-known semi-implicit pressure linked equations (SIMPLE) algorithm of Patankar<sup>13</sup> is used. These, in turn, enable one to correct the velocity field and improve the initially assumed pressure field. More information about the partial differential equations used in the analysis is given elsewhere<sup>5</sup>. For all post processing of the computed results, FAST animation software<sup>14</sup> has been used.

### 2.2. Computed wind flow field

*Single building model.* Figure 1 shows the streamline plots obtained from the simulation of a single building using four different grid systems. These plots (two-dimensional) show the side view pattern of the flow distribution for a section that is passing through the building center under normal flow conditions. The plots are obtained using the converged velocity components  $u$  and  $w$ . In the four figures, the computer model clearly predicted the flow separations from the windward edge and recirculation behind the building. To quantify these changes, the length of recirculation is calculated as explained in Vasilic Melting<sup>15</sup>. The edges of the recirculation zone are at points where the ratio of the  $w$ -component of the velocity to free-stream velocity takes a value close to zero,  $w/U_s \approx 0$ . The respective recirculation lengths have been found to be equal to  $1.5L$ ,  $2.3L$ ,  $2.2L$  and  $2.1L$  for the four grid systems:  $(38 \times 20 \times 28)$ ;  $(58 \times 26 \times 36)$ ;  $(68 \times 30 \times 40)$  and  $(78 \times 36 \times 40)$ . The length of recirculation increases with increase in the number of nodes and shows approximately a constant value for the third and fourth grid set. Nevertheless, to support this description of the expected flow behavior, experimental evidence of flow over buildings, such as flow visualization techniques are necessary. The influence of the other computational parameters such as computational domain size and the criteria used for convergence are examined and a diagnostic system is also developed, as explained in Baskaran and Stathopoulos<sup>8</sup>. Similar procedures are used in modeling the following configurations.

*Two building model.* The wind flow pattern between parallel buildings is one of the interesting and most often practically encountered problems. The buildings form as the two beds of a channel along which the air flow is passing. This particular wind induced effect is named the 'channeling effect'. The channeling effect phenomenon modifies the local wind flow in the passage between the buildings

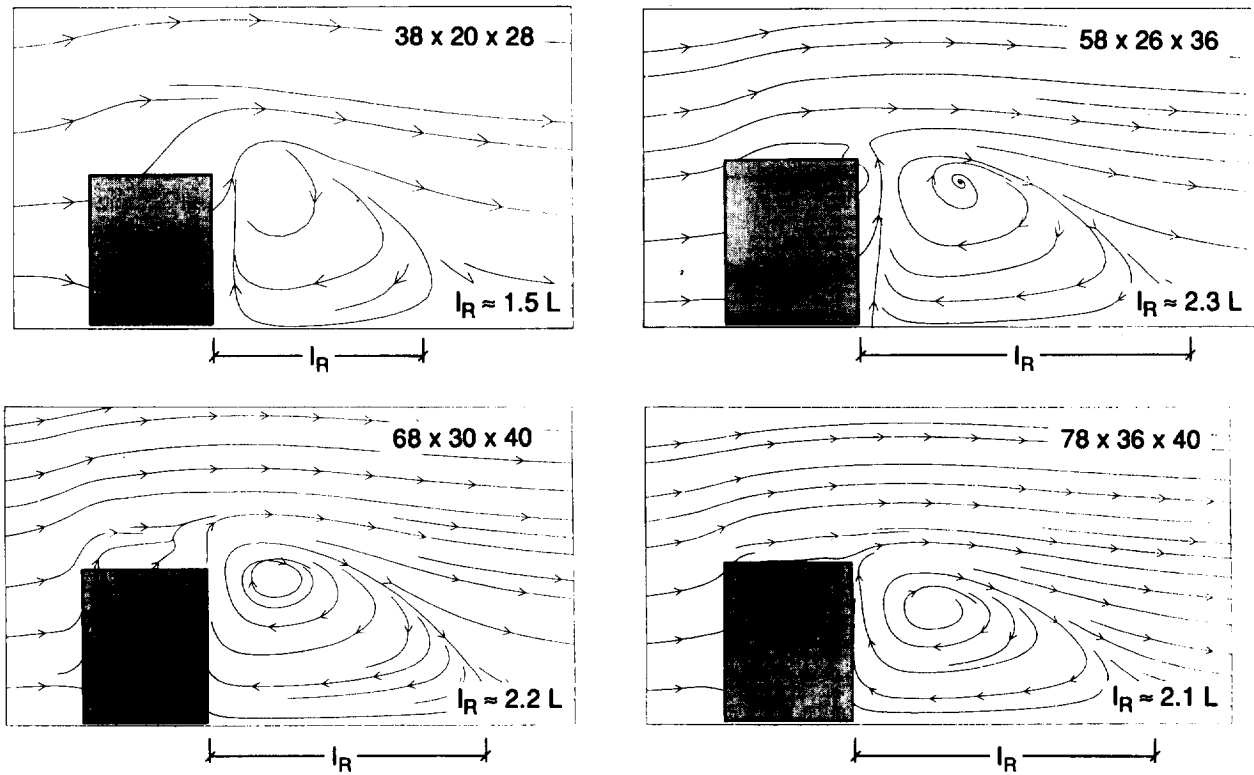


Figure 1 Computed air flow around a building with different grid arrangements

and creates unpleasant and sometimes dangerous wind environmental conditions. Various experimental investigations were carried out to understand the problem and guidelines are also formulated based on the measured wind tunnel data.

To model such a configuration using the CFD technique, two buildings having the same height and variable passage width ( $I = 6, 8$  and  $10$  m) are considered. Results are shown in Figure 2 in the form of vectors and stream line plots

taken at  $2$  m from the ground level. The formation of a channeling effect due to the increase of the flow field in the passage and recirculation behind the two buildings is clearly shown in the figure. Figure 3 displays the effect of the passage width on the predicted wind flow conditions around the buildings. To quantify the changes in the local wind environmental conditions, the calculated velocities are converted into conventional velocity ratios. These ratios are obtained by dividing the magnitude of the computed velo-

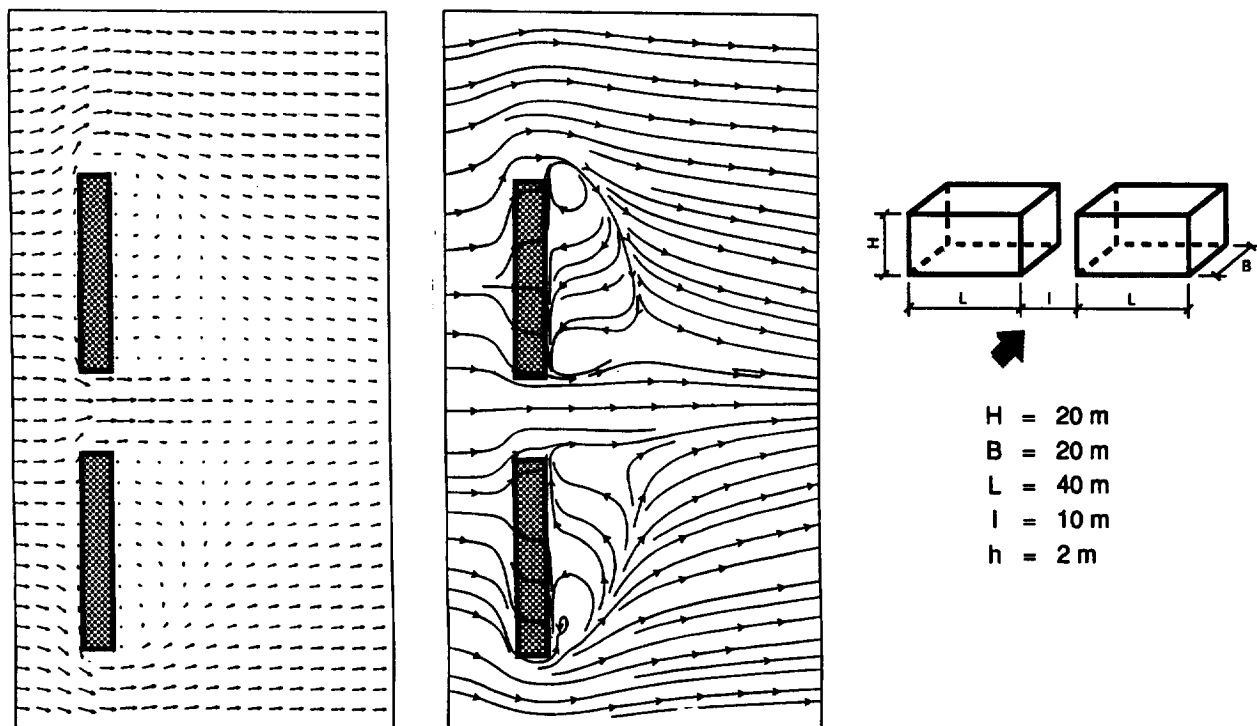


Figure 2 Velocity vectors and streamline plots of air flow between two buildings

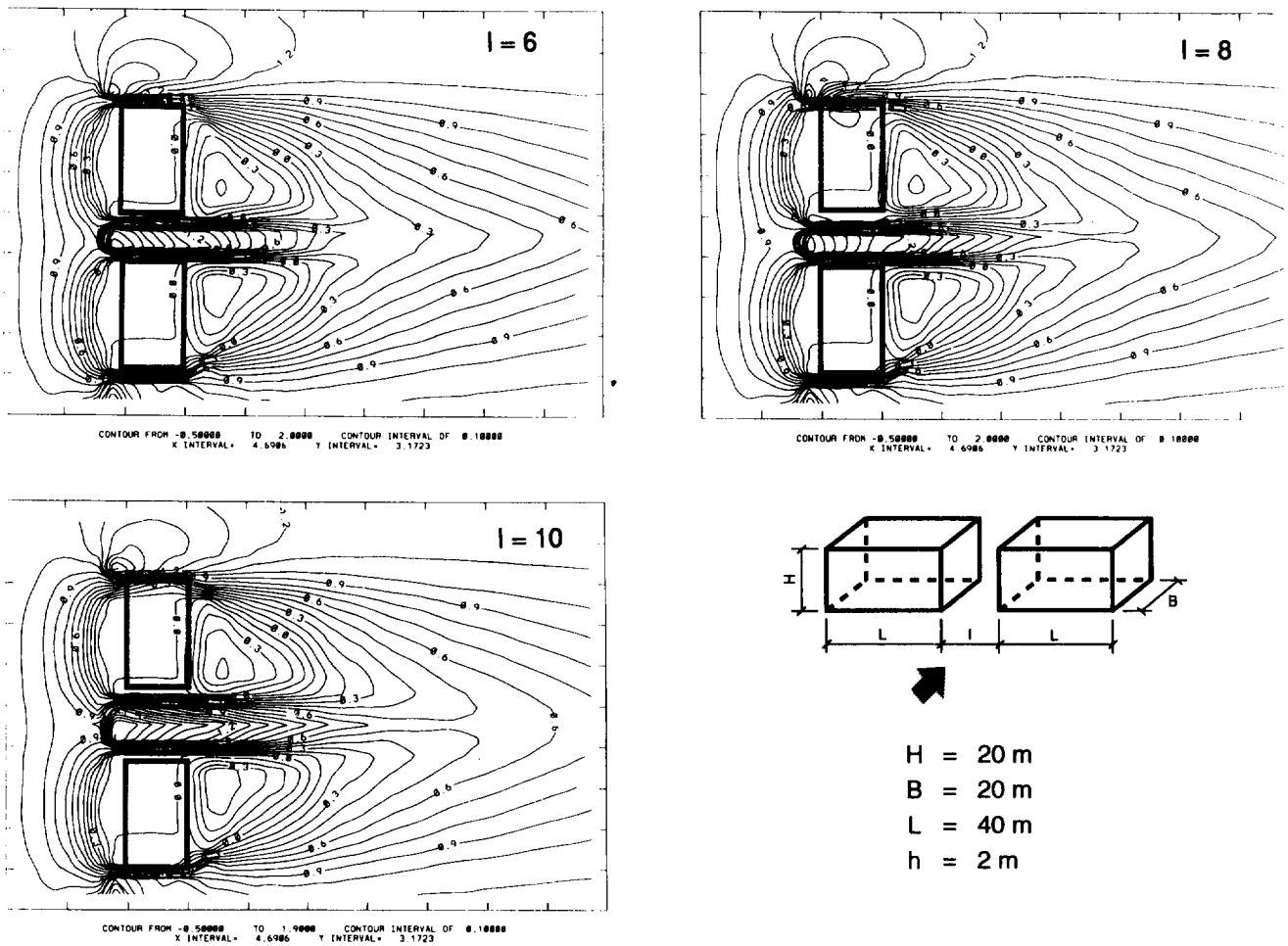


Figure 3 Effect of passage width between two buildings on velocity ratios

cities by the velocities in the absence of the buildings (free stream velocities). Since the velocities are taken at the same height for a particular location, these ratios will directly indicate the influence of the buildings on the local wind conditions. Values greater than unity indicate an increase in the velocity, on the other hand, ratios less than one indicate a reduction of local velocity. These ratios can be further used to evaluate pedestrian comfort around buildings. The velocity ratios (amplification or reduction factors) are shown in Figure 3 for three passage widths. The magnitudes of the ratios are higher along the passage and the building corners in comparison to the other locations. For points that are in high complex recirculating flow regions, the values are less than unity.

**Multiple building model.** To expand the modeling capabilities, further complexities have been considered in the simulation. Figure 4 shows the three-dimensional grid system of a multiple building arrangement for normal wind flow conditions. By changing the height of the individual buildings or the distances between them, one can easily model a variety of building arrangements. This is one of the reasons for selecting such an arrangement. Another equally important concern is the availability of the measured wind velocities around the buildings for this arrangement. Wiren<sup>16</sup> provides details of the wind tunnel experimentation. By incorporating the same inlet velocity and turbulence intensity profile conditions, simulations are performed for normal and oblique wind conditions.

Selection of the size of the computational domain to model such configuration depends mainly on the expected air flow patterns and wakes around the buildings under investigation. Air flow, in turn, depends on building dimensions and local terrain configuration. Researchers have commonly determined the size of the domain as a multiple of building dimensions<sup>17</sup>. It should also be kept in mind that the increase in the domain not only increases the number of grid nodes, but also demands more CPU time. Therefore, one must appropriately select the size of the domain so that a certain level of accuracy is maintained. By selecting several computational domains, sensitivity studies were carried out, as described by Baskaran<sup>5</sup>. At the end of the analysis, the dimension of the selected computational domain is shown in Figure 4. It has the following dimensions for the normal wind flow condition: in the  $z$  direction; up-stream distance ( $USD$ ) = 480 m, and down-stream distance ( $DSD$ ) = 1440 m; in the  $x$ -direction, distances to side, ( $DS1$ ) and ( $DS2$ ) are equal to 960 m and in the  $y$ -direction, distance to top, ( $DT$ ) = 108 m. Calculations have been made over  $55 \times 23 \times 49$  control volumes and the nodes are denser surrounding the building vicinity. As discussed before, a different computation domain is selected for the oblique flow modeling.

Figures 5 and 6 show the plan view of the computed velocity fields around the buildings at 2 m from the ground level for normal and oblique flow conditions, respectively. Only those vectors in the buildings proximity are displayed to get a closer and clearer insight of the flow conditions in

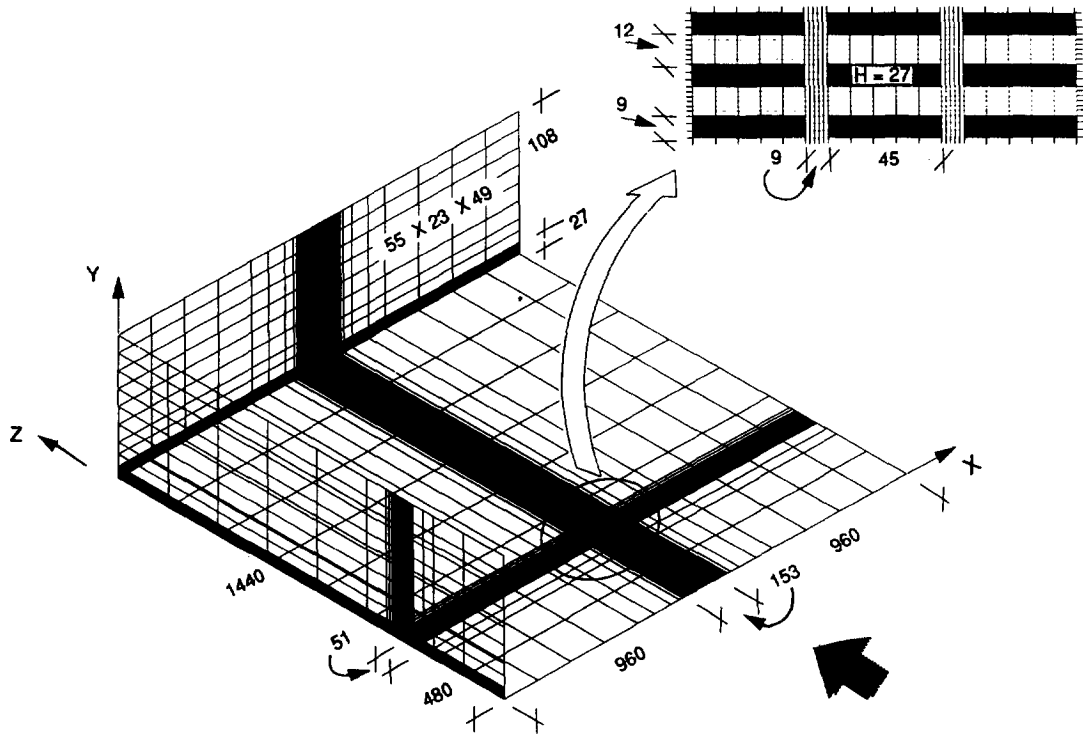


Figure 4 Three-dimensional grid arrangement for normal wind flow in modeling the multiple building configuration

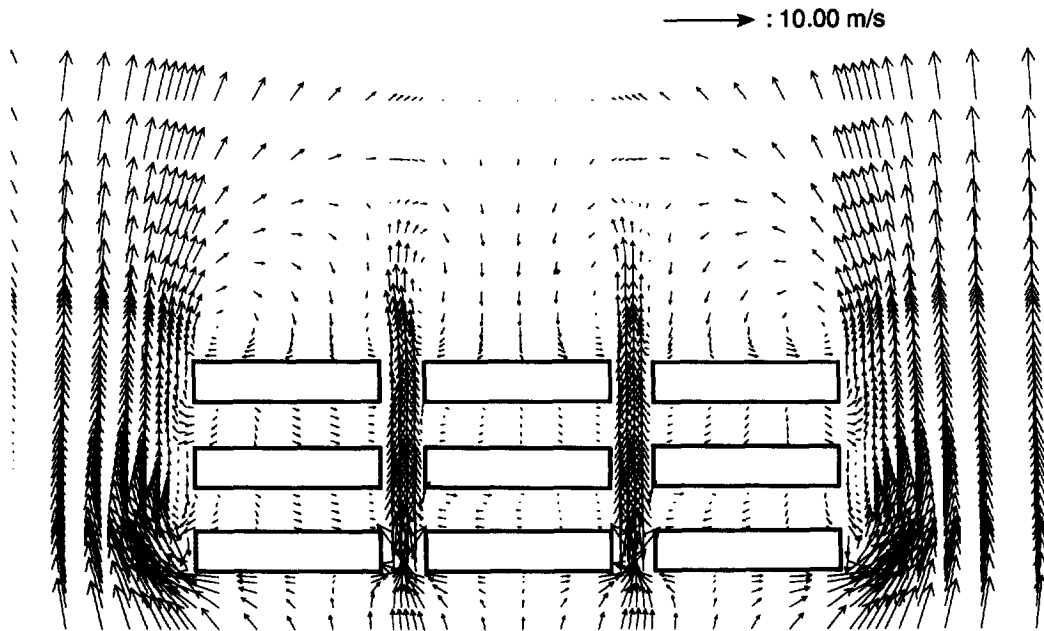


Figure 5 Velocity vectors around multiple building configuration for normal wind flow

the vicinity of the buildings. These two-dimensional velocity plots are obtained from the resultant of the longitudinal ( $w$ ) and lateral ( $v$ ) components using a reference velocity of  $10 \text{ m s}^{-1}$ . In these figures, the longer the vectors, the higher the wind speed. Flow separation points, changes in wind direction along the two sides of the buildings and the wake regions are clearly shown in the figure. This kind of vector plot is useful as preliminary information for the

designer, architect or engineer. Quick derivation by the computer and flexibility in incorporation of changes can stimulate enthusiasm about the computer evaluation of wind effects on buildings as opposed to the traditional wind tunnel modeling approach.

Comparing Figures 5 and 6, one can easily identify the wind directionality effects on the local flow developments. Some of them are grouped below:

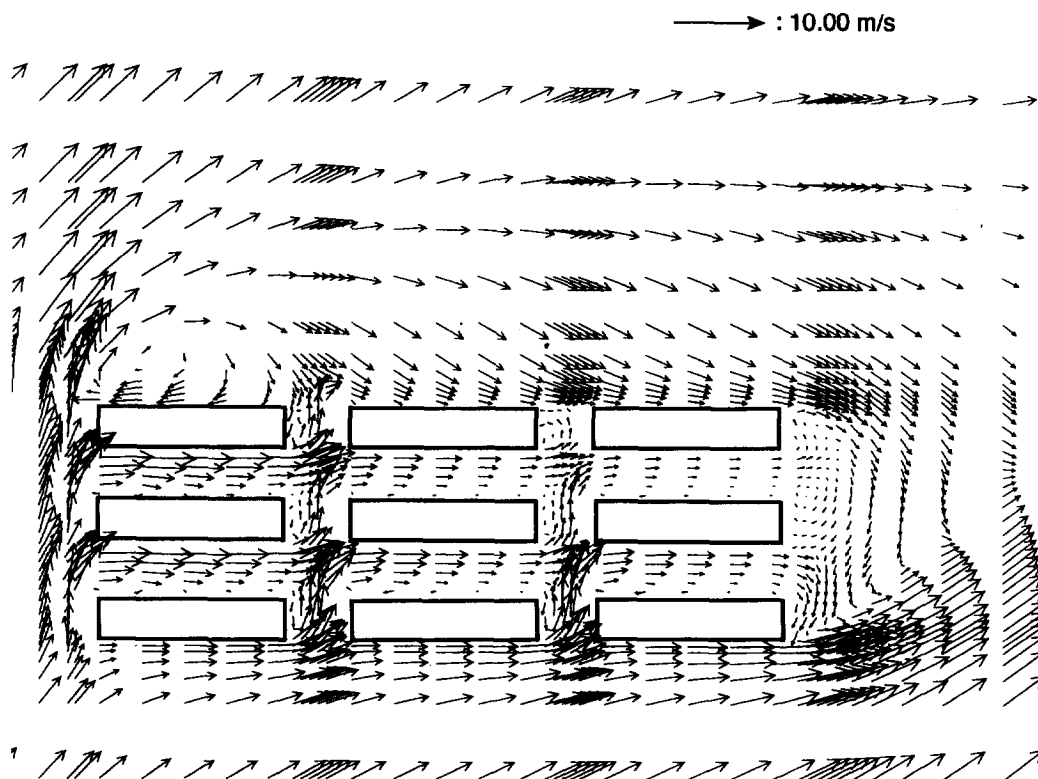


Figure 6 Velocity vectors around multiple building configuration for oblique wind flow

- symmetrical condition exists along the flow direction only for the normal flow;
- the lengths of the vectors are long, or wind speeds are high along the direction of the flow and thus the channelling effect is clearly predicted by the model for the normal wind condition;
- in comparison to the normal flow, velocities are high between the buildings (along the  $x$ -direction) for the oblique wind;
- for normal wind, reverse flow is formed between the buildings; and
- recirculation formed at the downstream side in the normal flow case (Figure 5) did not occur for the oblique wind case.

### 3. Model validation

Model validation forms an integral part of model development. A validated model can be used as a predictive tool during the design process to perform parametric studies. For the present study, model validation is achieved through systematic comparisons of the simulated results with the experimental data which are obtained from wind tunnel measurements. This in turn will enable us:

- to compare model predictions for different building configurations;
- to evaluate the model sensitivities for different boundary conditions (note that in modeling these different configurations, the wind tunnel inlet profile conditions are used as the boundary condition for the model); and
- to account for the different wind tunnel measurement techniques.

Wind tunnel studies have been carried out by Couhin<sup>18</sup>, Ishizaki and Sung<sup>19</sup>, Melbourne and Joubert<sup>20</sup>, Penwarden<sup>21</sup>, Wiren<sup>22</sup>, Isyumov and Davenport<sup>23</sup>, Gandemer<sup>24</sup>, Murakami *et al.*<sup>25,26</sup> and Stathopoulos and Stoms<sup>27</sup> to evaluate the pedestrian wind environmental conditions. Most of these measured data are for single building configuration and they have been compared with the simulated results by TWIST<sup>5,7,8</sup>. For other buildings configurations, however, only limited data is available in the literature. Review of the literature to acquire reliable measured velocity data for the different simulated configuration, reveals the need for a systematic experimental study to collect velocity data around the building for the purpose of benchmarking the model. Similar need was also recognized by Summers *et al.*<sup>28</sup> who measured the details of the flow field around a cube and compared with their simulated data.

Four wind tunnel studies are selected for model validation. They used different reference velocities to normalize the measured velocities around the buildings. For consistency in the comparison of wind tunnel data and computed results, first, the mean velocity ( $U$ ) is obtained using the three computed velocity components ( $U = \sqrt{u^2 + v^2 + w^2}$ ). Second, the same reference velocity of the wind tunnel studies is considered for normalizing. This can either be velocity at a gradient height ( $U_g$ , velocity at 2 m level ( $U_2$ ), velocity at 10 m level ( $U_{10}$ ) or velocity at any altitude and it is denoted in the comparison figures by  $U_n$ . The important features of the model validations are presented below.

#### Two building model

Stathopoulos<sup>27</sup> measured wind velocity and turbulence condition in a passage between two rectangular buildings. Experimental data for open country exposure with power

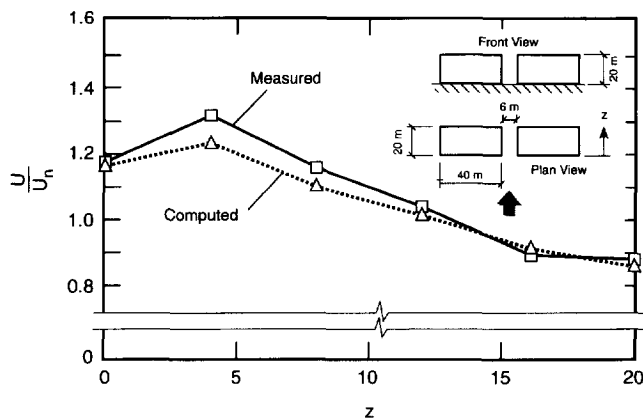


Figure 7 Model validation in predicting the channeling effect between two buildings

law exponent coefficient ( $\alpha$ ) as 0.15 and normal wind flow condition are used for the comparison. Simulation uses a mean speed profile having an exponent of 0.15 and a maximum turbulence intensity of 20% near the ground. The buildings are separated by a 6 m passage between them. Figure 7 shows a typical comparison of the model predictions with the experimental data. The results agree fairly well for locations along the passage center line. A correlation coefficient of 0.98 has been calculated showing about 2% deviation between the experimental data and computed values.

Having the two building model, one can conveniently change the geometry of the buildings and the passage width between them. Typical comparisons of such simulations are shown in Figure 8. Computed ratios are shown in points along with the wind tunnel traces. Simulations are performed with the same experimental conditions as Wiren<sup>21</sup>. Increase in the passage width increases the velocity ratios. Due to flow contraction, the velocity ratios are maximum at the entrance of both passage widths. It is evident that the model is sensitive to the geometrical changes of the building as well as the variations of the passage width.

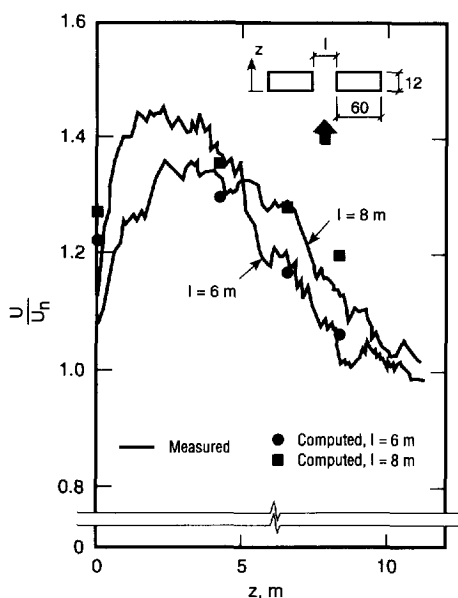


Figure 8 Model validation in predicting the channeling effect between two buildings for different passage width

Ishizaki and Sung<sup>19</sup> measured the development of the vertical flow between two buildings at three different elevations, the bottom ( $h_1$ ), the middle ( $h_2$ ) and top ( $h_3$ ). Figure 9 presents the model validation in predicting the vertical flow variation. In this figure, the  $x$ -axis presents the normalized values of the passage width ( $I$ ) with respect to the length of the building ( $L$ ), whereas the  $y$ -axis presents the velocity ratios. The ratios are maximum near the ground so is the difference between the computed velocities and measured data. Nevertheless, for locations further away from the ground, the agreements are better between the measured data and computed results.

#### Multiple building model

Model validation is also performed for a multiple buildings configuration and presented in Figure 10 for normal wind flow conditions. Four typical locations ( $y/B = -0.30, 1.9, 4.2, 5.8$ ) are considered. For an example  $y/B = -0.30$  represents the upstream separated flow characteristics, whereas  $y/B = 5.8$  presented the downstream wake flow characteristics. The other two locations represent the cross flow characteristics. In Figure 10, for all locations, two peaks occurred along the passage. Also, the model clearly produced the expected symmetrical conditions on either side of  $x/L = 1.6$ . The velocity ratios are decreasing moving from upstream to down stream, namely, from  $y/B = -0.3$  to  $y/B = 5.8$ . The predictions are compared to experimental data produced by Wiren<sup>16</sup>. Wiren<sup>16</sup> performed extensive wind tunnel measurements and grouped the measured velocity ratios in the form of contour plots for various wind directions. Due to the symmetrical condition, the measurements were performed for only half of the arrangement. From the contour plots, local velocity ratios are extracted and presented in Figure 10. In general, compared to the measured data, the computed ratios are higher along the passage and smaller for other locations. Average deviation between computed and measured data is about 5%.

Figure 11 examines the model predictions, in a similar format as Figure 10, for oblique wind flow conditions. As shown, significantly different velocity ratios are computed for oblique wind flow conditions. The symmetrical conditions are diminished due to changes in the incoming flow direction. At the upstream ( $y/B = -0.3$ ), the flow is dominant along the  $x$  direction having two peaks along the passage. For other locations, through flow along the  $x$  direction is observed. This can be easily seen from the decrease of velocity ratios as  $x/L$  increases. Moreover, the available measured data from Wiren<sup>15</sup> show good agreement with the computed ratios.

## 4. Application of the model for a design case study

The following are the results from an application of the developed model for the investigating of wind environmental conditions of the actual site. The model has been used as a predictive tool in arranging the different building locations during the design stage of the following site.

### 4.1. Modeled configuration for the case study

Figure 12 shows an aerial view of the investigated site and the surroundings. There are three proposed buildings BLDG1, BLDG2 and BLDG3. The local landscape is composed of a sloping hill on the south side of the investigated

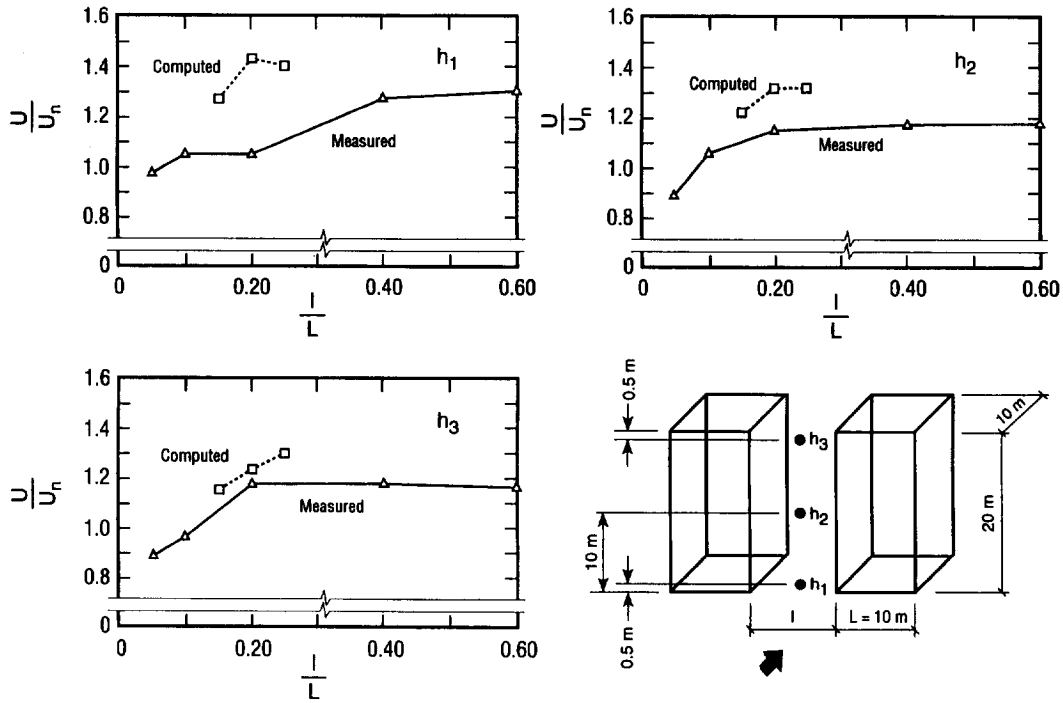


Figure 9 Model validation in predicting the vertical flow variation between two buildings

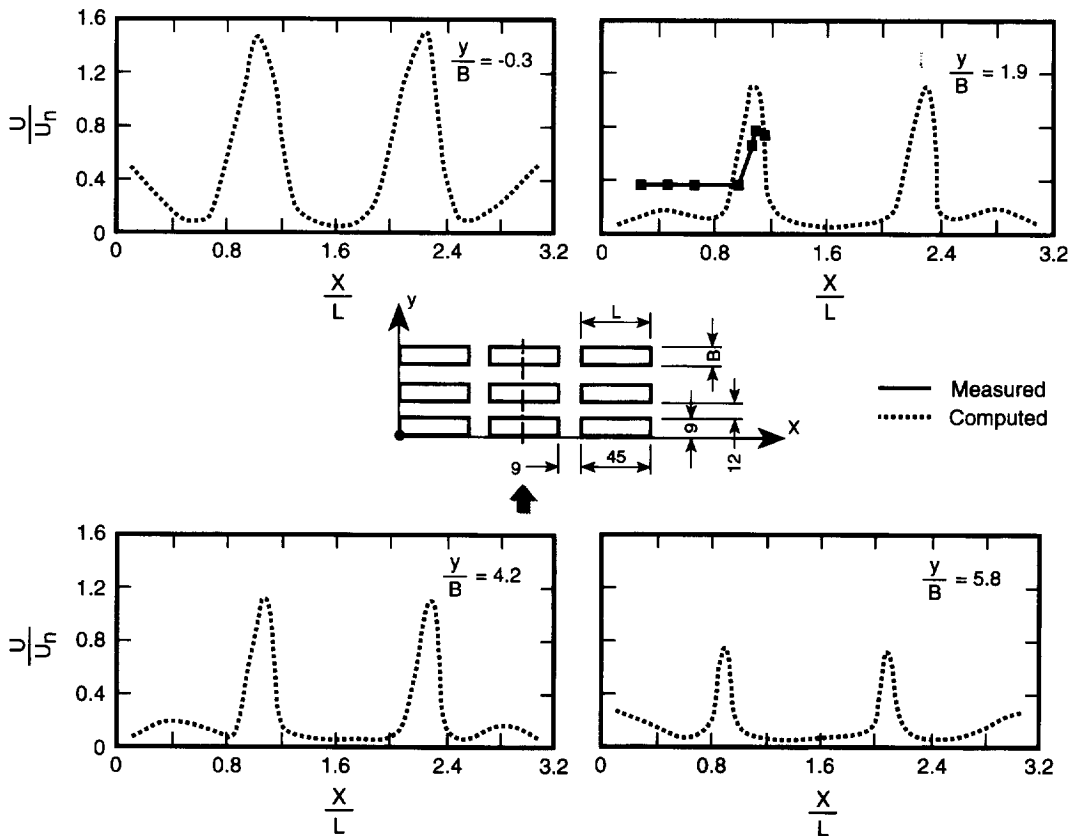


Figure 10 Model validation in predicting the flow around multiple building configurations (normal wind)

buildings as well as the trees around the buildings. Keeping the building BLDG1 location constant along with the local landscape, buildings BLDG2 and BLDG3 are placed at several locations to investigate their effect on BLDG1. The investigated building BLDG1 is about 112 m long, 24 m width and three stories high and therefore the building

aspect ratios are unusual, 5 and 10, respectively, for length/width and length/height. There is a 'step cutting' at the third floor that adds to the complexity of the building shape. Due to this unusual aspect ratio and complex building shape, evaluation of the local wind environmental condition is warranted.



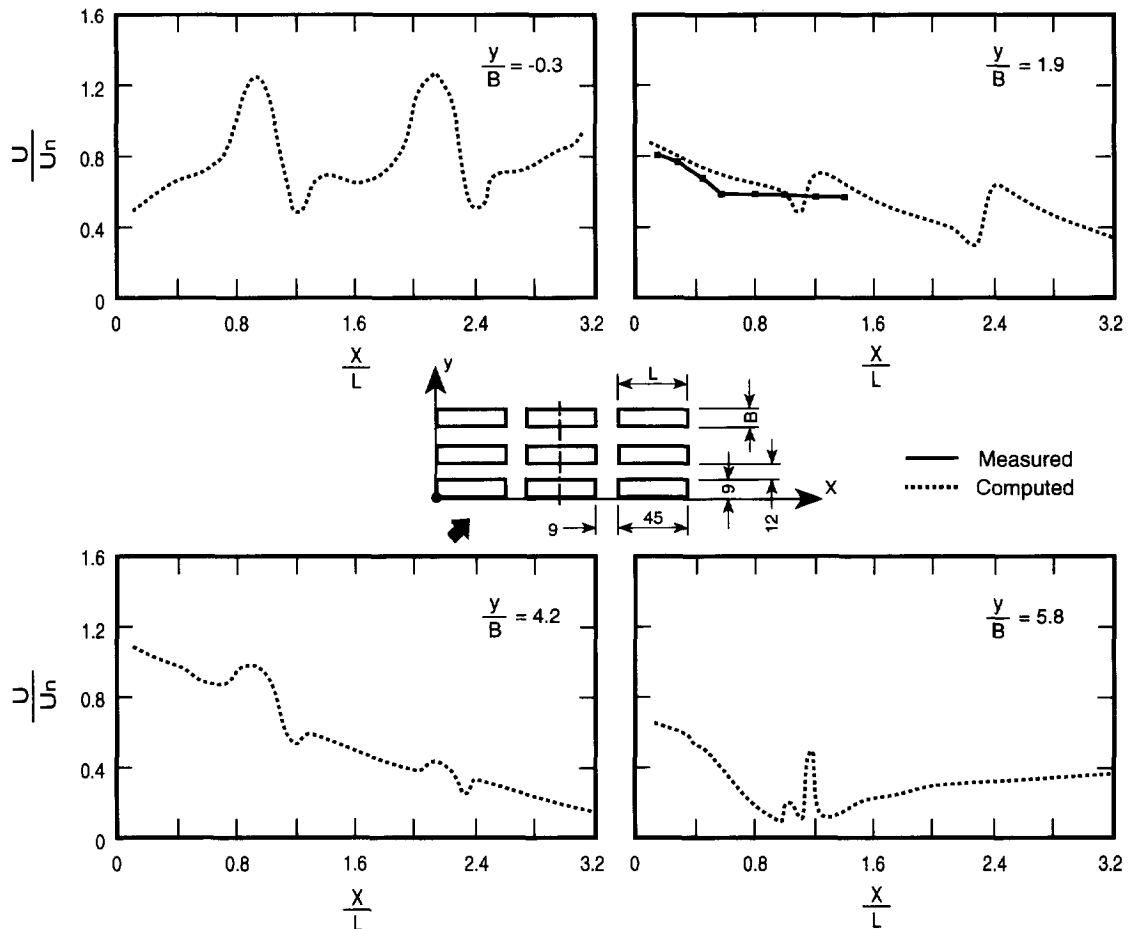


Figure 11 Model validation in predicting the flow around multiple building configurations (oblique wind)

In Figure 13, the dotted line represents the 'proximity region'. The term 'proximity region' defines an area surrounding the BLDG1 building and significantly affects the behavior of air flow around the building. The boundaries of this region are determined such that buildings or natural obstacles outside this area will not significantly affect the nature of air flow around BLDG1. Thus the proximity region is dependent on the local terrain rather than the direction of the wind. As shown in Figure 13, for the NE wind direction, the computational domain has the following dimensions:  $USD = 300$  m;  $DSD = 900$  m;  $DT = 50$  m;  $DS1$  and  $DS2$  are equal to 290 m. For the case where the wind blows from the west direction, these distances are, respectively:  $USD = 340$  m;  $DSD = 688$  m;  $DT = 50$  m;  $DS1 = 490$  m and  $DS2 = 750$  m.

For computer modeling purposes, the geometry of the buildings, inside the proximity region, is transformed from the actual site by defining their boundaries using a set of points with known coordinates. For modeling the local terrain, a tree has been simulated using 50% porous wall. The 50% porosity reveals the actual density between the trees due to the natural arrangement of trees. On the other hand, the hill has been modeled using two-step prisms on top of each other in elevation as shown in Figure 13. The two-step prisms are inclined on the plan view to match the actual landscape.

#### 4.2. Animated turbulent air flow fields

The model under development is three-dimensional and the fluid properties are computed and stored at various special locations. One effective approach to investigate the special variation of fluid property is through flow visualization. Through computer visualization, various aspects of the numerical solution, which would otherwise be difficult to identify experimentally, may easily be observed. Engineers and researchers are thereby able to gain a much better insight into the behavior of the corresponding numerical solution. Data visualization can be achieved in many ways, ranging from simple two-dimensional color-shaded graphs to complex three-dimensional animation. A very powerful system can perform real-time animation by developing successive frames from raw data and displaying them. In a less powerful system the raw data is first generated and stored in plot files and animation is performed by rapidly displaying the pre-developed frames in a pre-defined sequence and with a pre-defined time interval. The latter method is under development for the numerical evaluation of wind flow conditions around buildings.

This section discusses the results obtained from the investigation of the all three discussed configurations. The principal velocity component,  $w$ , and kinetic energy  $k$  are extracted from the simulated results to evaluate the changes in the environmental conditions of the local wind. The  $k$

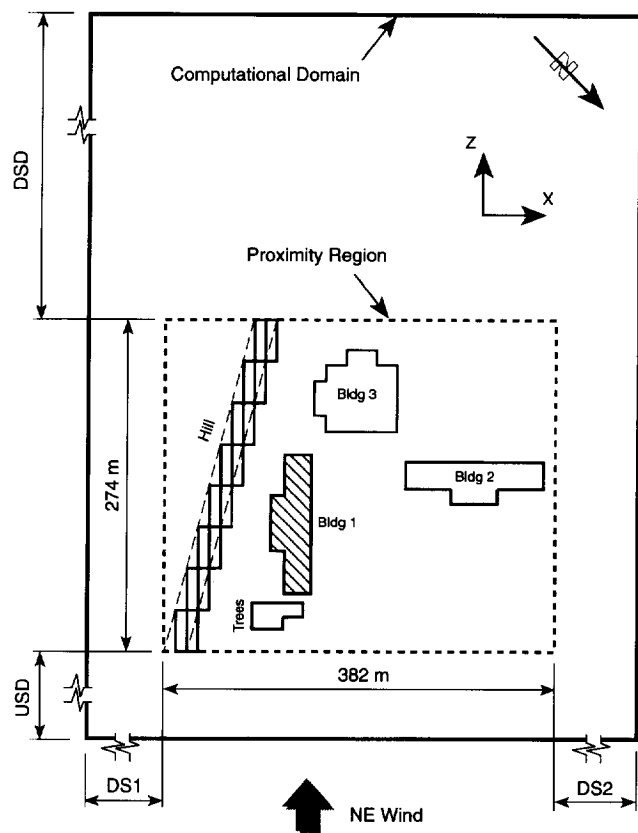


Figure 13 Computational domain, proximity region and buildings modeled for the case study

values are further converted into percentages of turbulence intensity by dividing the square root of  $k$  by the free stream velocities,  $U_s$ , i.e.  $\sqrt{k}/U_s \times 100$ .

Using FAST<sup>14</sup>, animations are performed to visualize and investigate the air flow conditions around the buildings. Animated images are recorded out to VHS video cassettes. For the presentation of the results in report form, images are selected from the animation and saved into TARGA file format. TARGA, abbreviated as TGA, is a particular file format for storing color graphic images. These files are further edited and printed in the form of color contour plots. Such plots are presented at two levels, namely 2 and 7.7 m above ground. The height of 2 m above ground represents a standard measurement commonly followed by the wind engineering researchers. The height of 7.7 m is the beginning of the third level 'step cutting' on BLDG1, representing a potential area for snow accumulation. These plots have four major colors: blue, green, yellow and red. The color spectrum from blue to red represents the increase in both the velocity components,  $w$ , and the turbulence intensity,  $I$ . This will facilitate the visualization of air flow conditions around the buildings. Analysis of this nature illustrates some of the inherent advantages in CFD modeling.

Figure 14 presents the  $w$ -component values around BLDG1 for the NE wind direction. Separation from the windward edge and recirculations and involved eddies behind BLDG1 are observed. Separation is represented by a yellow color in which there is change in the flow direction with respect to the incoming flow. The edges of the recirculation zone are at points where the ratio of the  $w$ -component of the velocity to free-stream velocity takes a value close to zero<sup>13</sup>,  $w/U_s \approx 0$ . In the figure, this may be identified

where the color changes from blue to green. For the present investigation, the length of the recirculation region is approximately 1.5 times the building height. Due to the unusual building length, a large disturbance region on the leeward side has also been observed during the analysis. This disturbance decreases with the increase in height. For example, comparing the images obtained for the 2 m height with those for 7.7 m, the flow disturbances are less significant at a height of 7.7 m than at a height of 2 m. This is not surprising because the only interaction affecting the flow at a height of 7.7 m is due to the building, whereas the flow field at the 2 m level will interact with both the ground and the building surfaces. Moreover, the dining hall, which is only 5.5 m high, does not significantly affect the flow.

Wind directionality effects are investigated and presented in Figures 15 and 16, respectively, for SW and W wind directions. Comparing Figure 14 with Figure 15, the wind direction has been changed by 180°. Although the overall wind environmental conditions are not symmetrically replicated in Figure 15, much of the explanation presented for Figure 14 applies equally to Figure 15. In Figure 16 for the westerly wind condition, BLDG1 is shielded by other buildings in the upstream direction and by the hill and trees in the downstream direction. This reduces the length of the recirculation region for BLDG1. Thus, the recirculation zone is more pronounced for the normal flow as opposed to the oblique flow. This has been found to be true at both 2 and 7.7 m heights above ground. The 'channeling wind effect' occurred between the building and hills at 7.7 m between the buildings BLDG1 and BLDG2 is also disturbed for the west wind direction.

Figure 17 shows the turbulence intensity images at 2 m height for all three configurations. In addition, the animated image for the configuration of the single building is also included for comparison purposes. Generally, the turbulence intensity increases with an increase of the obstruction in the flow domain. This has been found to be true for the present investigation. The overall turbulence intensity values are amplified when the surrounding buildings are included in the computer simulation. It is evident from Figure 17 that maximum turbulence intensity increased from 15 to 25% when other buildings and landscapes were considered in the model. On the other hand, the extension of the turbulence intensity region around BLDG1 is decreased. This is due to the shielding effect caused by other buildings near BLDG1.

## 5. Conclusions

A considerable effort has been invested in applying and validating CFD techniques for air flow around: single, double and multiple building configurations. From the preceding discussions, the following conclusions can be made:

- (1) CFD is emerging as a powerful tool for the investigation of building air flow applications;
- (2) CFD techniques can provide very detailed predictions of air velocities around buildings;
- (3) model validation, forming an integral part of model development, indicated that the CFD techniques can qualitatively predict the flow around various building configurations;
- (4) extensive literature review revealed that the availability of reliable experimental data is limited for model benchmarking purposes;



Figure 12 Aerial view of the site for the case study

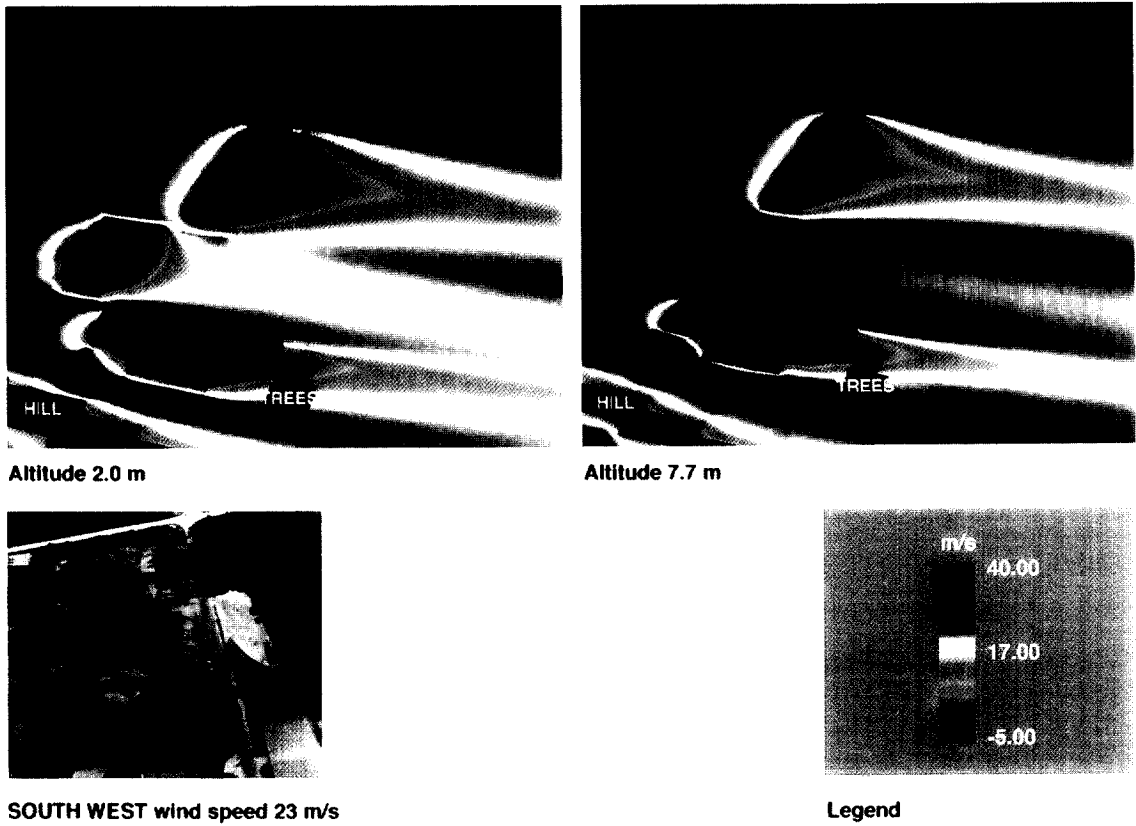


Figure 14 Animated contour images of w component velocity—NE wind

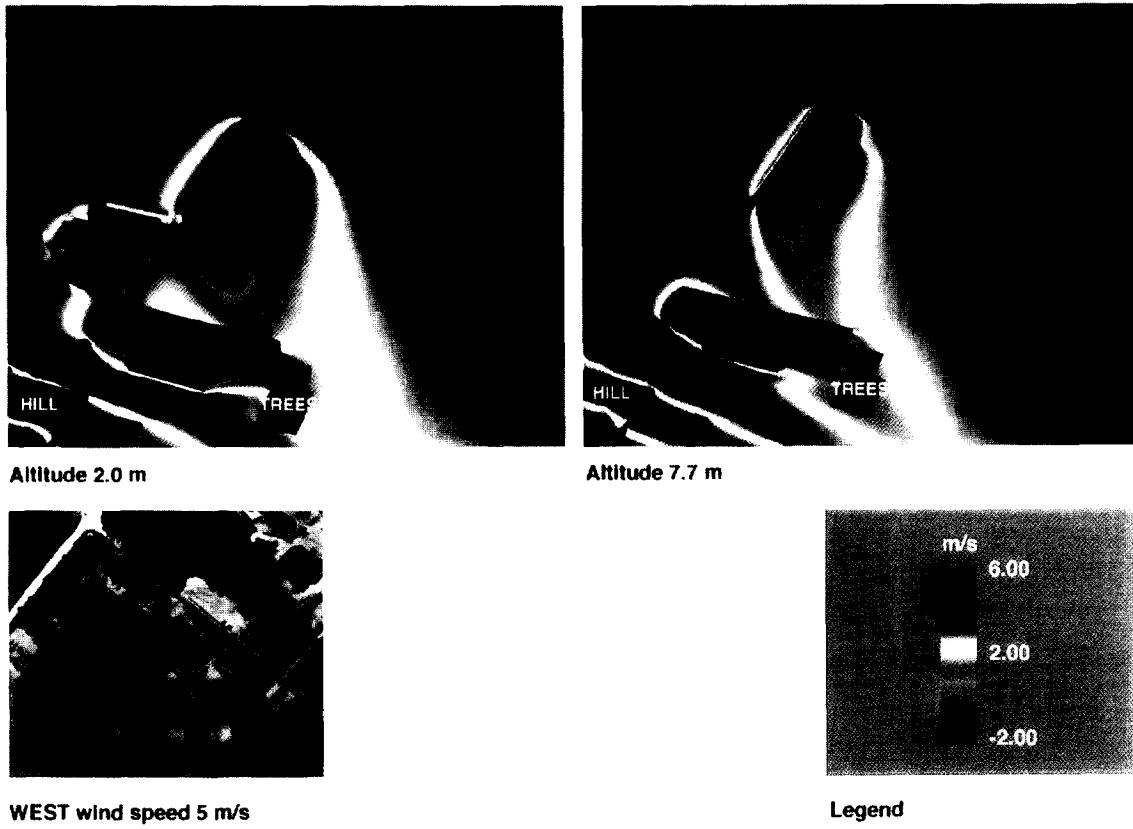


Figure 15 Animated contour images of  $w$  component velocity—west wind

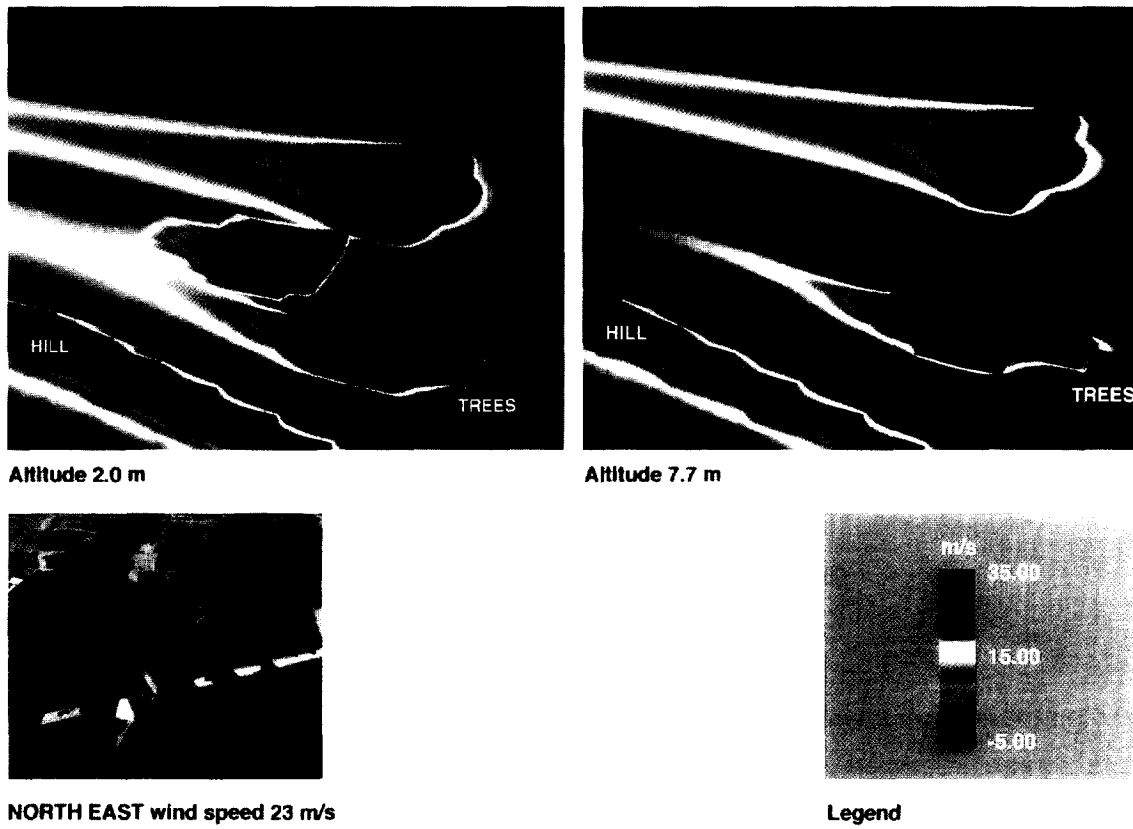


Figure 16 Animated contour images of  $w$  component velocity—SW wind

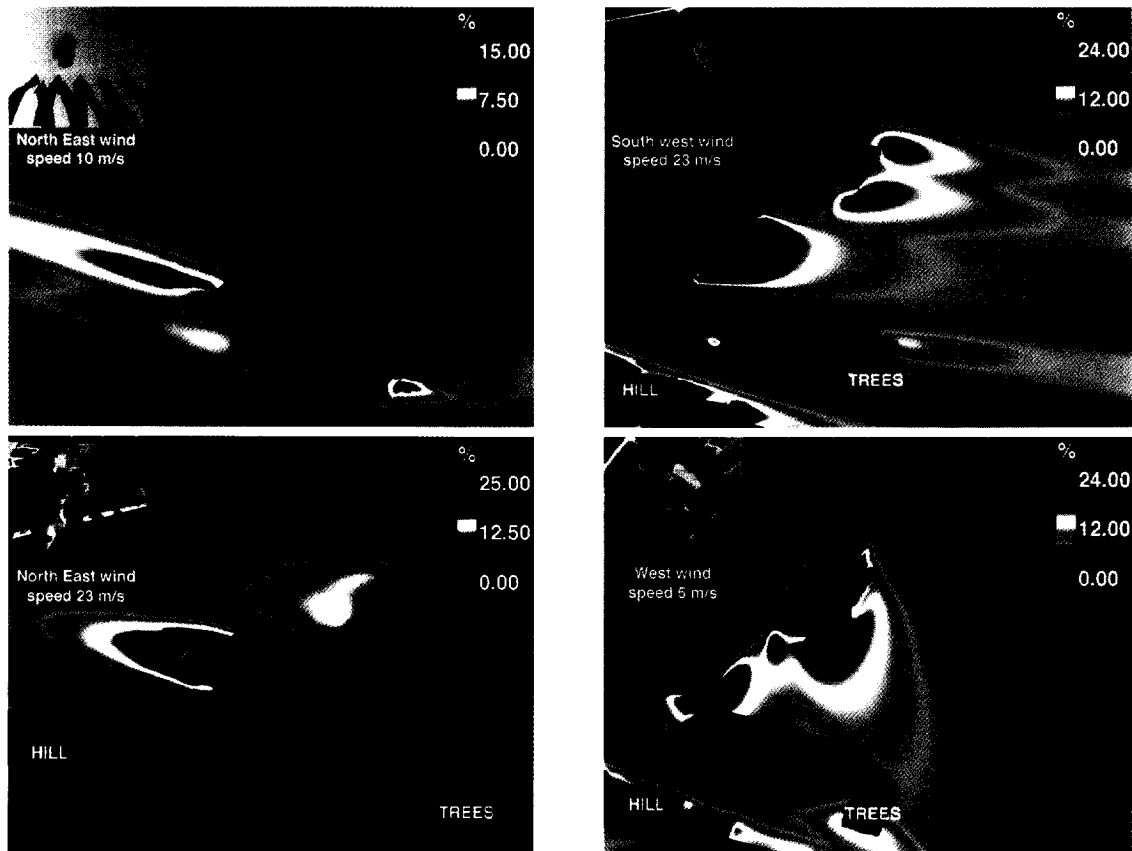


Figure 17 Animated contour images of turbulence intensity for various wind directions



- (5) applying the CFD techniques for the case study and visualizing the wind flow field around buildings provided various design opportunities for the owners and developers;
- (6) it must be emphasized that it is vital that proper engineering judgment be exercised in applying and interpreting the output obtained from the CFD models.

### Acknowledgments

The authors wish to thank Mr F. Pelletier, Government Services Canada, for allowing us to present their results of the case study and for their contribution in the preparation of the animated color images. The authors would like to acknowledge the encouragement and advice provided by T. Stathopoulos, Concordia University, during the first stage of the work described in this paper.

### References

- 1 Cermak, J. E. 'Wind-simulation criteria for wind-effect tests'. *ASCE J. Struct. Div.* 1984, **110**, 328–339
- 2 Davenport, A. G., Isyumov, N., King, J. P. C., Novak, M., Surry, D. and Vickery, B. J. 'BLWT II: the design and performance of a new boundary layer wind tunnel', *Proc. 5th U.S. National Conf. on Wind Engineering*, Lubbock, Texas, 1985, 2A–35–2A–40
- 3 Cermak, J. E. 'Advances in physical modeling for wind engineering', *ASCE, J. Engng Mech.* 1987, **113**, 737–757
- 4 Whitbread, R. E. 'Model simulation of wind effects on structures', *Proc. Wind Effects on Buildings and Structures*, London, 1965, pp. 182–196
- 5 Baskaran, A. 'Computer simulation of 3D turbulent wind effects on buildings', Ph.D. thesis, Concordia University, Montreal, Canada, 1990
- 6 Baskaran, A. and Stathopoulos, T. 'Computational evaluation of wind effects on buildings', *J. Bldg Environ.* 1989, **24**, 325–333
- 7 Stathopoulos, T. and Baskaran, A. 'Boundary treatment for the computation of 3D turbulent conditions around buildings', *J. Wind Engng Ind. Aerodyn.* 1990, **35**, 177–200
- 8 Baskaran, A. and Stathopoulos, T. 'Influence of computational parameters on the evaluation of wind effects on the building envelope', *J. Bldg Environ.* 1993, **27**, 39–49
- 9 Baskaran, A. and Stathopoulos, T. 'Prediction of wind effects on buildings using computational methods—state of the art review', *Can. J. Civ. Engng* 1994, **21**, 805–822
- 10 Spalding, D. B. 'A general purpose computer program for multi-dimensional one and two-phase flow', *Math Comput. Simulation* 1981, **XXIII**, 267–276
- 11 Baskaran, A. 'A numerical model to evaluate the performance of pressure equalized rainscreen walls', *J. Bldg Environ.* 1994, **29**, 159–171
- 12 CHAM Development Team, *The PHEONICS—1.6.6 user guide*, CHAM, Wimbledon, London, 1989
- 13 Patankar, S. V. 'Numerical heat transfer and fluid flow', Hemisphere, McGraw-Hill, New York 1980
- 14 Walatka, P. P. *FAST maps—user interface—FAST Beta 2.1*, NASA Ames Research Center: WAO and RND, April 1992
- 15 Vasilic-Melling, D. 'Three dimensional turbulent flow past rectangular bluff bodies', Ph.D. thesis, Imperial College of Science and Technology, London, 1977
- 16 Wiren B. G. 'A wind tunnel study of wind speeds near the ground in a group of block-type buildings', Research report TN:23, The Natural Swedish Institute for Building Research, Sweden, 1991
- 17 Beranek, W. J. 'General rules for the determination of wind environment'. *Proc. 5th Int. Conf. on Wind Engineering*, Fort Collins, USA 1989, Vol. 1, pp. 225–235
- 18 Counihan, J. 'An experimental investigation of the wake behind a two-dimensional block and behind a cube in a simulated boundary layer flow', Central Electricity Research Laboratories, Note no. RD/L/N 115/71, June 1971
- 19 Ishizaki, H. and Sung, I. W. 'Influence of adjacent buildings to wind', *Proc. 3rd Int. Conf. on Wind Effects on Buildings and Structures*, Tokyo, Japan, 1971, pp. 145–152.
- 20 Melbourne, W. H. and Joubert, P. N. 'Problems of wind flow at the base of tall buildings', *Proc. Wind Effects on Buildings and Structures*, Tokyo, 1971
- 21 Penwarden, A. D. 'Acceptable wind speeds in towns', *Bldg Sci.* 1973, **8**, 259–267
- 22 Wiren, B. G. 'A wind tunnel study of wind velocities in passages between and through buildings', *Proc. 14th Int. Conf. on Wind Effects on Buildings and Structures*, Heathrow, UK, 1975, pp. 465–475
- 23 Isyumov, N. and Davenport, A. G. 'The ground level wind environment in built-up areas', *Proc. Wind Effects on Buildings and Structures*, London, 1975
- 24 Gandemer, J. 'Wind environment around buildings: aerodynamic concepts', *Proc. Wind Effects on Buildings and Structures*, London, 1975
- 25 Murakami, S., Shoda, T., Goto, T. and Uehara, K. 'Experimental studies about strong wind effects on pedestrians: walking tests in large wind tunnel', *J. Inst. Ind. Sci.*, University of Tokyo, 1976, 277–286
- 26 Murakami, S., Uehara, K., Goto, T., Shoda, T. and Yamada, M. 'Wind effects on pedestrians; part II walking tests in precinct in front of high-rise buildings', Report of the Annual Meetings of Architectural Institute of Japan, 1977
- 27 Stathopoulos, T. and Stoms, D. 'Wind environmental conditions in passages between buildings', *J. Wind Engng Ind. Aerodyn.* 1986, **24**, 19–31
- 28 Summers, D. M., Hanson, T. and Wilson, C. B. 'Validation of a computer simulation of wind flow over a building model', *J. Bldg Environ.* 1986, **21**, 97–111